Journal of Bangladesh Institute of Planners ISSN 2075-9363
Vol. 5, December 2012, pp. 151-167, © Bangladesh Institute of Planners

Spatial Analysis of Land Surface Temperature in Dhaka Metropolitan Area

Debasish Roy Raja*

Abstract

The research is carried out to assess the relationship between the land surface temperatures (LST) and land cover (LC) changes both in quantitative and qualitative ways in Dhaka Metropolitan Area (DMA) using Landsat TM/ETM+ data over the period 1989 to 2010. Supervised classification methods have been taken to prepare the LC map. LST is derived from the thermal band of Landsat TM/ETM+ using the calibration of spectral radiance and emissivity correction of remote sensing. GIS based spatial simulation has been conducted to establishing this relationship using NDBI and NDVI. The changing of LST is directly correlated with LC transition. LST is increasing in those areas where urban developments have been concentrated over this period. Besides, the amount of Vegetation (NDVI) is negatively correlated with LST. The trend of the LST and LC transition indicates that LST will be abruptly increased in the near future and it will affect on micro climate. The urban LST maps, the analyses of thermal-land cover relationships and the spatial simulated figure could be used as a guideline for urban planning, strategies for quality improvement of urban environment and a smart solution to the reduction of UHI effect.

Introduction

Dhaka city is confronted with a significantly high rate of physical and population growth since 1981 (BBS, 1997; BBS, 2003), which has created tremendous pressure on urban land, utility services, and other amenities of urban life. A substantial growth of built-up areas (*urban development)* is transforming increasingly the landscape from natural cover types to Impervious Surface (IS). It is building up Urban Heat Island (UHT), which has adverse effect on the *urban climate change* such as abrupt temperature rise, erratic rainfall, degrading air quality(Mayer et al, 2003; Ifatimehin *et al*, 2010; Hossain, 2008; Atkinson, 2002; Dewan *et al*, 2009; Alam and Rabbani, 2007 and Dixon and Mote, 2003). Therefore, Dhaka city is affected by erratic rainfall and heat stress, resulting calamities like flood, water logging, health outbreak, and water scarcity including greenhouse climate changes. The 0.5^0 C global warming realized over the last century is due mainly to the increase of greenhouse gases, urbanization, and other plausible climatic factors such as desertification (Alam and Rabbani, 2007; Nasrallah and Balling, 1993; Kukla *et al*, 1986 and Wood, 1988). However, only few *qualitative* studies (Ahmed, 2008 and Basak, 2006) were found to assess the urban climate change in Dhaka city but *no study* has been performed yet to correlate the changes of both Land Cover Area (LCA) and Land Surface Temperature (LST) with urban development and Vegetation. Therefore, it is undoubtedly important to examine the relationship between urban development and vegetation and land surface temperature (LST) in Dhaka city and find out its consequences in the future.

Objectives and Methodology

The study is to examine the impacts of urban development and vegetation on land surface temperature (LST) in Dhaka city with two specific objectives:

* Assistant Professor, Department of Urban and Regional Planning, Chittagong University of Engineering and Technology (CUET), Chittagong, Email: rajabuet@yahoo.com

a) To determine LST changes over different LCA in Dhaka city over different time-periods using remote sensing and spatial techniques of GIS

b) To study the impact of urban development (NDBI) and vegetation (NDVI) on LST

To achieve the research objective, Landsat Satellite images of DMA area over different time periods (1989, 2000 & 2010) is compiled from USGS website as zip format. Landsat satellite images have been chosen, because it has thermal band from which LST would be determined as well as different period of images are available in free public-domain. The main limitation of this kind of image is low spatial resolution which is 30m. For better result of this research, year of 1989, 2000 and 2010 images are chosen, which are of the same season, but have low seasonal variation. Another limitation of the study is collection of reference data for Classification. The details of the Landsat data for analysis are shown in Table 1. The Landsat TM/ETM+ image is collected as Universal Transverse Mercator (UTM) within 46N- Datum World Geodetic System (WGS) 1984.

In this research, the Dhaka Metropolitan Area (DMA) is selected for study because of its high level growth in the last two decades (Rabbani, 2010) as shown in Figure 1. DMA covers the core Dhaka city as well as its surroundings areas. The changing land surface temperature (LST) with change of land cover (LC) is also considered for the surrounding areas of DMA.

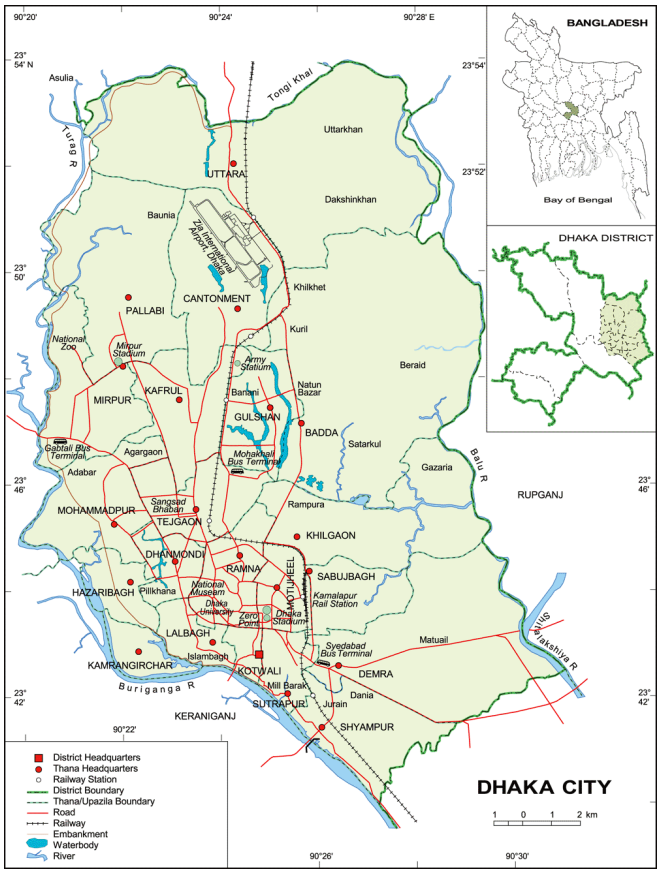

Source: Bangla Pedia , 2012

Fig. 1: Location map of the study area

Table 1: Landsat TM/ETM+ images used in the study

Representative year	Path and Row	Date & Scan time	sensor	Weather	Resolution	Cloud %	Remarks
1989	137 & 44	Jan 12, 1989 03:57:14	Landsat4-5 TM	Normal	30m	0	Low seasonal variation
2000	137 & 44	Feb 28, 2000 04:17:27	Landsat7 ETM+	Normal	30m	0	
2010	137 & 44	Jan 30, 2010 04:15:40	Landsat4-5 TM	Normal	30m	0	

Source: US Geological Survey, 2012

Land Cover Map Preparation

To prepare LC map image enhancement is necessary tool to identify and select the interest area. Image can be enhanced in several ways, such as Contrast Enhancement, Intensity/ hue/ saturation transformations, Density slicing etc. Landsat image also can be enhanced by generating composite band combination. Generation of composite band combination such as false color Composite (FCC), true color composite, false natural color composite etc. are used for this research.

Composite Band Combination

Landsat TM/ETM+ image has several bands. Any of three (3) bands of the same sensor are formed an image that is called as false color composite (FCC) (NASA, 2008). In the Figure 2, several composites of Landsat 5 TM images (DMA, 2010) are shown using different band combinations. RGB means basic three color read, green and blue and it has been used for band 4, 3 and 2 to make false color composite (FCC). This FCC usually shows the urban area as blue, vegetation as read, water bodies as Dark Blue to black, soil without vegetation as white to brown. In the same way, true color composite shows the different land cover as its real color. Trafficability composite (RGB= Band 6, 4 & 3) emphasize the traffic lane and built-up area as dark purple color. So different land cover features can be separated by choosing color of the cell. More color intensity also increases the probability of any land cover types of the composite image. These band composite images are used to identify and select the interest area for building the signature of image classification. Different false color composites (FCC) maps with any three bands of dhaka city for the year 2010 are shown in Figure 2 (a. True Color Composite, b. False Color Composite, c. False Color Composite, d. False Natural Color Composite, e. Traficability Composite).

Image Classification

Image classification is a process of sorting pixels into a finite number of individual classes, or categories, of data based on their values (Erdas, 2006). In this study, supervised classification method has been used. The steps of this method are described in the following categories.

Building Signature

The composite band images are used to digitize the know land covers so that the signature value can be collected. Signature values contain the DN (Digital Number) value of each band of this image such as the reflectance value of the cell. It is called signature development. For this research, 5 (five) types of land cover have been selected on the basis of their similar character

shown in Table 2. Lots of signature vale is determined for each land cover types and a statistical mean value can also be derived for each land cover from this value. This is called combine signature or merge signature.

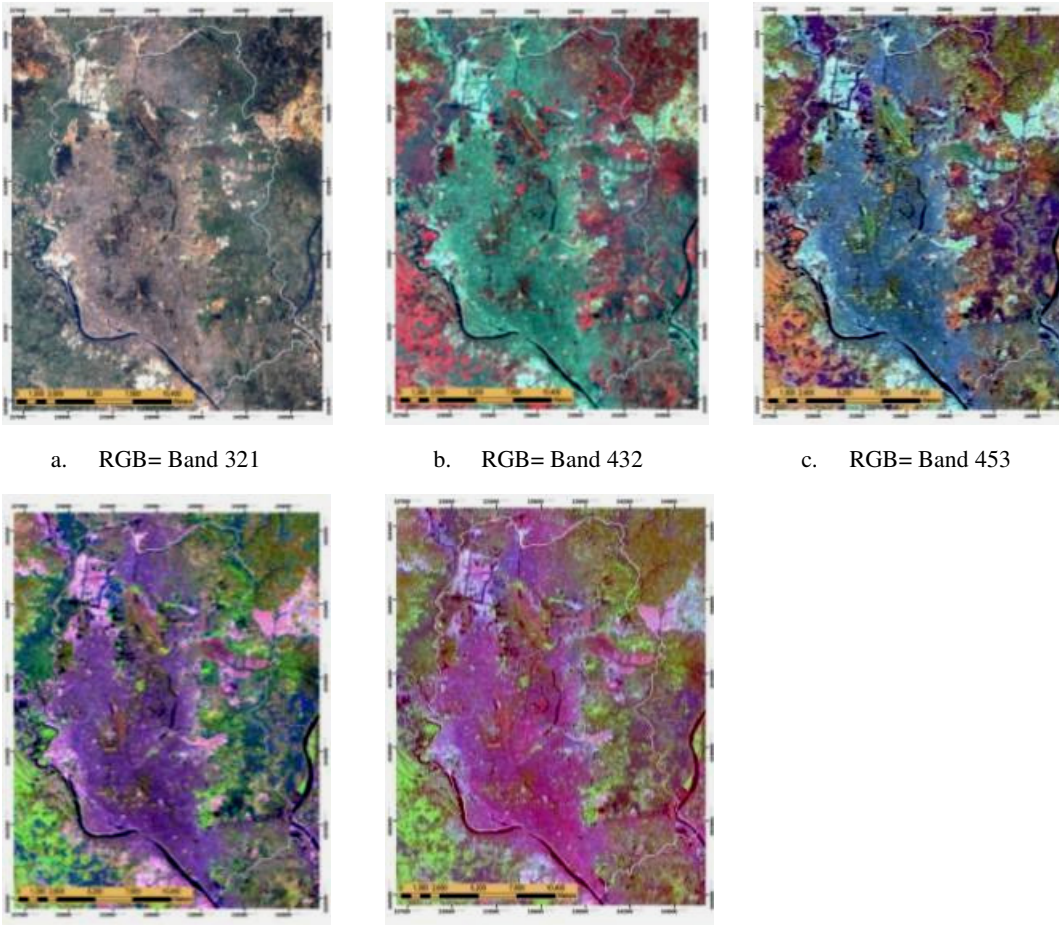

a. RGB= Band 321 b. RGB= Band 432 c. RGB= Band 453

d. RGB= Band 543 e. RGB= Band 643

Source: Produced by Author
Fig. 2: Composite Band Combination

Table 2: Selected criteria for land cover classification

LC type	Criteria
Water & wetland	River, Permanent open water, pond, canal, lake, reservoir, permanent and seasonal wetland
Vegetation Type	Trees , agricultural land, grassy land, park and playfield etc.
Built-up Area	All type of infrastructure such as residential, commercial , industrial, road, village settlement etc.
Earth Fill or Sand	Constructions site , development land, earth filling or sand
Bare soil	low land, , marshy land, vacant land

Evaluation of Signature

While signature values are collected from the composite band image, there may be deviation or error. It can be evaluated from the signature mean graph. The signature value range of each land cover types is separated from others. From the combine signature mean graphs (Figure 3), it is also found that each land cover type mean signature value is different from others. Though the difference of Land cover type signature mean value is close for one band but in other band the difference is found high.

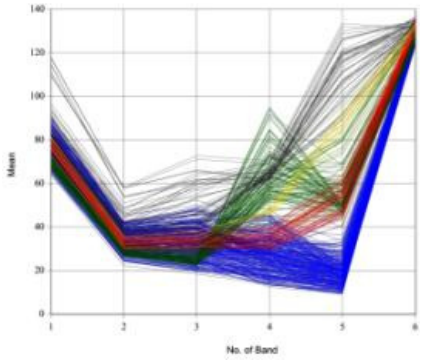

Signature mean graph (1989)

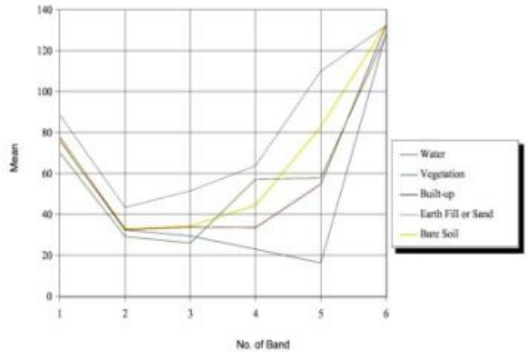

Combine Signature mean graph (1989)

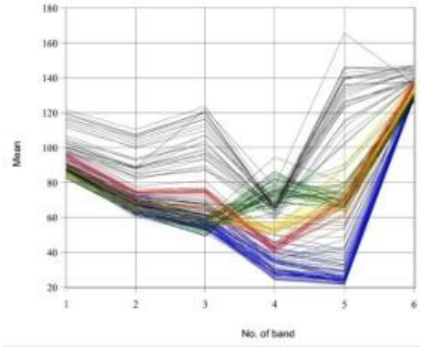

Signature mean graph (2000)

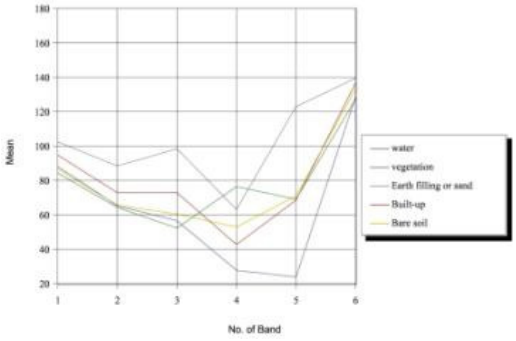

Combine Signature mean graph (2000)

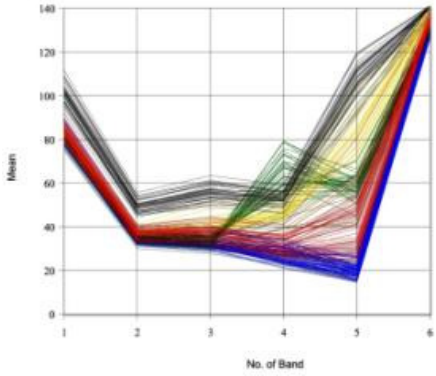

Signature mean graph

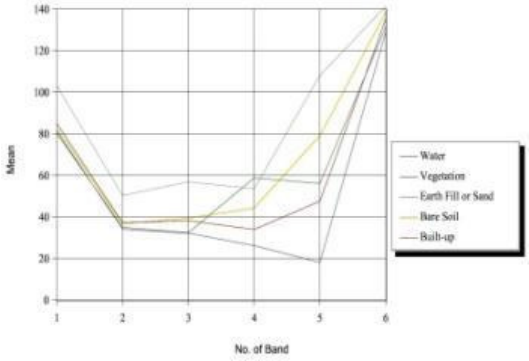

Combine Signature mean (2010)

Fig 3: Signature mean graph according to different band

Classification with Maximum Likelihood of Parametric Rule

The image is classified using the developed signature. The supervised classification techniques are divided into two groups: non-parametric and parametric procedures. For this research, maximum likelihood of parametric rule is used for classification as it provides an estimate of overlap areas based on statistics. A parametric method of supervised classification is based on statistical parameters (e.g., mean and covariance matrix) of the pixels. Maximum likelihood classification considers not only the mean or average values in assigning classification, but also the variability of brightness values in each class. The maximum likelihood decision rule is based on the probability that a pixel belongs to a particular class. The classified images of different years are shown in the Figures 4, 5 and 6.

Error Estimation

The map accuracy is derived from the signature error matrix. The map accuracy is given in the Table 3. From the table it is found that the selected signatures are not overlapped with other signature. At least 95% of the each class data are accurate for all year. The overall accuracy is about 99.60% for 1989, 98.28% for 2000 and 99.32% for 2010.

Table 3: Signature Error estimation

Year 1989						
Classified Data	Reference Data					
	Water (%)	Vegetation (%)	Earth fill (%)	Built-up (%)	Bare soil (%)	Row Total
Water	99.91	0.03	0.00	0.00	0.00	28618
Vegetation	0.06	98.64	0.00	0.00	2.68	5981
Built-up	0.02	0.00	99.74	0.00	0.85	3411
Earth Fill	0.00	1.33	0.00	98.71	0.73	470
Bare soil	0.01	0.00	0.26	1.29	95.73	801
Column Total	28641	6023	3408	389	820	39281
Year 2000						
Classified Data	Reference Data					
	Water (%)	Vegetation (%)	Earth fill (%)	Built-up (%)	Bare soil (%)	Row Total
Water	97.13	0.00	0.00	0.01	0.00	6829
Vegetation	0.16	98.77	0.00	0.00	0.38	10927
Earth fill	0.00	0.31	100.00	0.00	0.00	1941
Built-up	0.46	0.00	0.00	97.70	0.44	10924
Bare soil	2.26	0.93	0.00	2.29	99.17	6996
Column Total	7030	11027	1907	11119	6534	37617
Year 2010						
Classified Data	Reference Data					
	Water (%)	Vegetation (%)	Earth fill (%)	Built-up (%)	Bare soil (%)	Row Total

Water	99.66	0.00	0.00	0.00	0.29	11593
Vegetation	0.07	98.76	0.00	0.18	0.40	3716
Earth fill	0.00	0.00	99.56	0.00	0.18	1584
Built-up	0.00	1.24	0.44	99.82	0.16	1181
Bare soil	0.28	0.00	0.00	0.00	98.97	7249
Column Total	11612	3723	1578	1118	7292	25323
Map accuracy (%)						
1989		**2000**		**2010**		
99.60%		98.28%		99.32%		

Source: Prepared by author

Conversion of Thermal Band of the Landsat TM/ETM+ to Land Surface Temperature

Conversion of the Image Digital Number (DN) Values to Spectral Radiance

Landsat TM/ETM+ image pixels are converted to units of absolute radiance using the following equations (NASA, 2008):

Radiance, $L\lambda$ = (QCAL/255) *((LMAX-LMIN) + LMIN (For Landsat TM)

Radiance, $L\lambda$ = ((LMAX-LMIN)/(QCALMAX-QCALMIN)) * (QCAL-QCALMIN) + LMIN (For Landsat ETM+)

Where: QCALMIN = Minimum Digital Number(DN) Value

QCALMAX = Maximum Image Digital Number(DN) value

QCAL = Digital Number(DN) of the Band 6

LMAX = Maximum spectral radiances

LMIN = Minimum spectral radiances

For conversion of Image digital number (DN) to spectral radiance following data is used shown in Table 4.

Table 4: Conversion of the image digital number (DN) values to spectral radiance

Value	Year		
	1989(TM)	2000 (ETM+)	2010 (TM)
QCALMIN	1	0	1
QCALMAX	255	255	255
QCAL	Image Digital Number	Image Digital Number	Image Digital Number
LMAX	15.303	17.040	15.303
LMIN	1.238	0.000	1.238

Source: Meta files of Landsat TM/ETM+ Image, USGS.

Spectral Radiance to Black Body Temperature

Satellite Brightness temperature or black body temperature is derived from spectral radiance by the following formula (NASA, 2008; Artis & Carnahan, 1982; Zhang *et al*, 2008).

$$T_B = \frac{K_2}{ln\left(\frac{K_1}{L_\lambda} + 1\right)}$$

Where

T_B = At- satellite Brightness temperature

L_λ = Spectral Radiance

Table 5: ETM+ and TM Thermal Band Calibration Constants

	K_1 (Wm^{-2} sr^{-1}µm^{-1})	K_2 (K)
TM	607.76	1260.56
ETM+	666.09	1282.71

Source : NASA, 2008

Emissivity Correction to Calculate Land Surface Temperature (LST)

The LST is derived from the following formula for emissivity correction. Each land cover types have different emissivity. For this study, a simple grouping, that is, 0.95 for vegetative areas and 0.92 for non-vegetative areas (Weng, 2001; Nichol e*t al.*, 1994) are used to calculate LST.

$$S_t = \frac{T_B}{1 + (\lambda . T_B/\rho) . ln\ \varepsilon}$$

Where

S_t = Land Surface Temperature

λ = 11.457µm

ρ= 1.438× 10^{-2} mK

ε= Emissivity

Derived LST map of different years are shown in Figures 4, 5 and 6. Table 6 shows the statistical information of LST.

Preparation of NDVI & NDBI

In remote sensing Normalized Difference of Vegetation Index (NDVI) has been used to measure density of vegetation. To measure the NDVI, following formula have been used for calculating this index value (Chen *et al.,* 2006).

NDVI = (band 4 - band 3)/ (band 4 + band 3)

Built-up area as well as impervious surface can be measured by Normalized Difference Built-up Index (NDBI). NDBI of different years are derived using the following formula (Zha *et al*, 2003).

NDBI= (band 5 - band 4)/ (band 5 + band 4)

The statistical information of NDVI and NDBI is provided in Table 6.

Table 6: Statistical Information of LST, NDVI & NDBI

Year	LST				NDVI			NDBI		
	Minimum	Maximum	Average	Standard deviation	Range	Mean	Standard deviation	Range	Mean	Standard deviation
1989	20.42	33.97	24.74	1.67	-0.63 to 0.65	0.155	0.139	-0.698 to 0.554	0.069	0.143
2000	22.02	39.47	28.26	2.44	-0.41 to 0.36	-0.087	0.131	-0.459 to 0.502	0.112	0.122
2010	21.82	36.13	26.81	2.17	-0.27 to 0.50	0.057	0.092	-0.488 to 0.588	0.087	0.137

Source: Produced by Author

LCA 1989

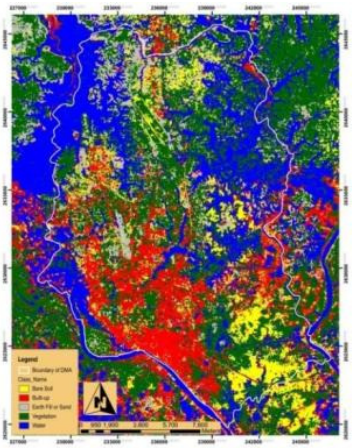

LST 1989

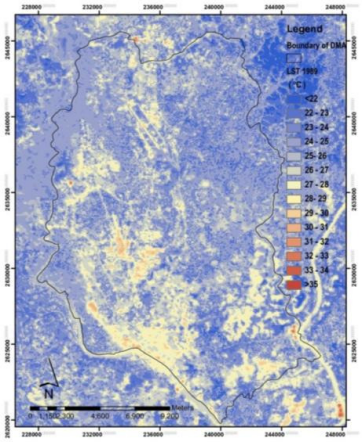

3

Source: Produced by Author

Fig. 4: LCA and LST MAP, 1989

LCA 2000

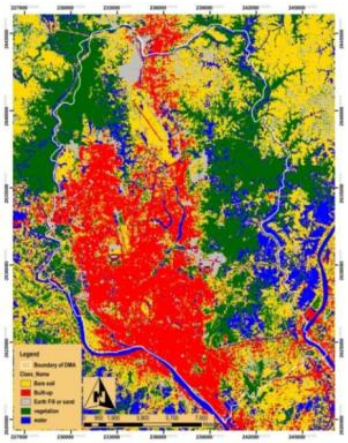

LST 2000

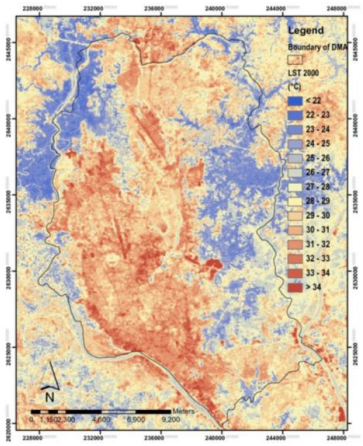

Source: Produced by Author

Fig. 5: LCA and LST MAP, 2000

LCA 2010

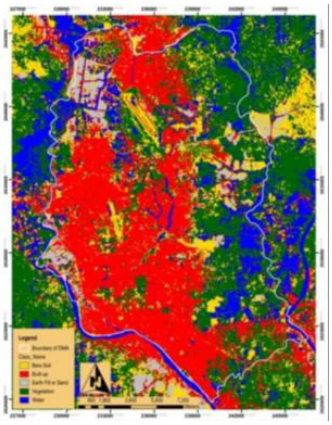

LST 2010

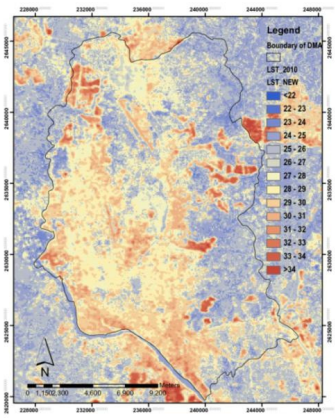

Source: Produced by Author

Fig. 6: LCA and LST MAP, 2010

Analysis and Results

Land Cover Change

Table 7 summarizes the land covers that have been changed during the period of 1989 to 2010. In 1989, the mentionable LC areas were vegetation and water body as 105.22 and 76.00 km² respectively, whereas only 59.39 km² was found as built-up area. In 2000, both vegetation and water bodies were decreased to 70.14 and 19.45 km² respectively and the built-up area was increased to 95.42 km². But the scenario is changed in 2010; the vegetation and water bodies are increased slightly as 5.82 % and 5.17 % respectively. It may have happened because of seasonal variation. But the growth of built-up area remains the same in increasing rate.

Table 7: Land Cover (LC) change in DMA (1989 to 2010)

Land cover types	Year			Loss & Gain of LC (1989 to 2010)		
	1989 (km²)	2000 (km²)	2010 (km²)	1989-2000 (%)	2000-2010 (%)	1989-2000 (%)
Water	76.00	19.45	35.17	-18.59	5.17	-13.42
Vegetation	105.22	70.14	87.85	-11.53	5.82	-5.71
Built-up	59.39	95.42	129.89	11.85	11.33	23.18
Earth fill or sand	30.53	32.36	15.09	0.60	-5.68	-5.08
Bare soil	33.01	86.79	36.15	17.68	-16.65	1.03
Total Area	304.15	304.15	304.15	-	-	-

The total scenario of changing land cover is shown in Figure 7 during the period of 1989 to 2010. During this period, the water body is decreased by 13.42% of total area, whereas the built-up area is increased by 23.18%.

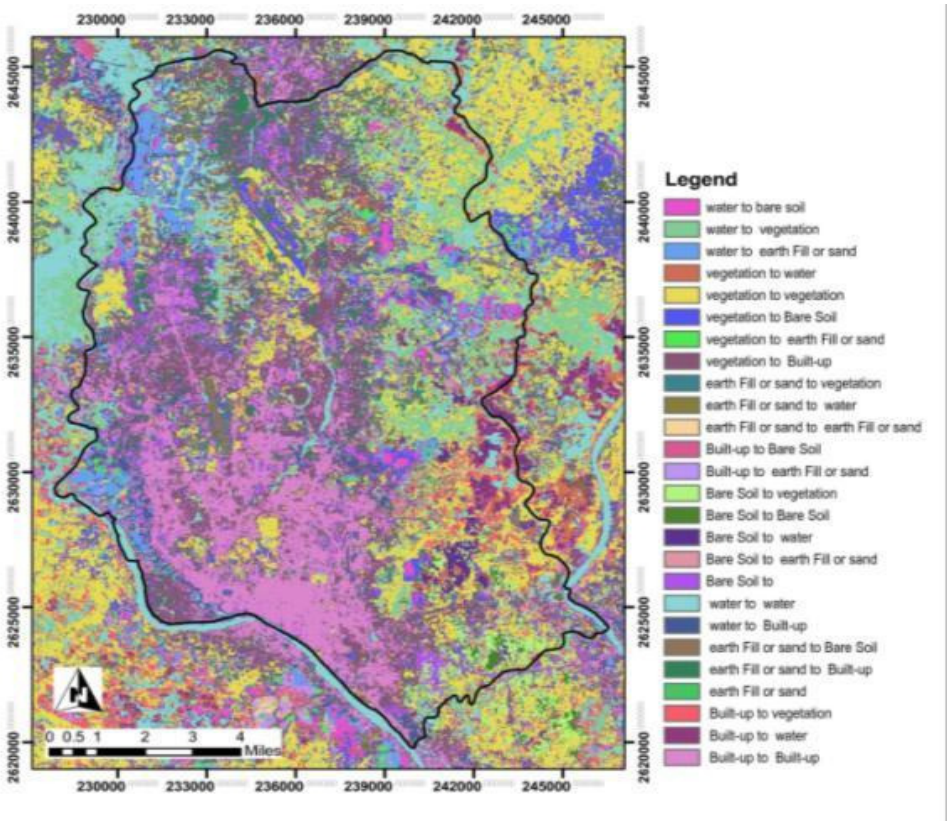

Fig. 7: Loss and gain of different Land Cover types (1989 to 2010)

Transition of Built-up Area

Figure 8 depicts how Built-up area has been grown up during the period of 1989 to 2010. An area of 30.17 km² and 11.00 km² of Vegetation and Bare Soil lands respectively have been turned into Built-up area during the year 1989 to 2000 as illustrated in Table 8 and Figure 8. In this decade, the highest amount of vegetation land has been converted into Built-up area in the south and east portions of the city as shown in Figure 8 (1989 to 2000) in green color.

Table 8: Conversion of Land Cover Types into Built-up area in DMA (1989 to 2010)

Land cover types	1989 (Km²)	1989 to 2000 (Km²)	2000 to 2010 (Km²)
Water to Built-up	-	4.9383	2.3643
Vegetation to Built-up	-	30.1716	8.2989
Built-up to Built-up	-	43.0254	85.6332
Earth fill or sand to Built-up	-	6.2793	11.7054
Bare soil to Built-up	-	11.0007	21.8862
Total Built-up Area	59.3874	95.4153	129.888

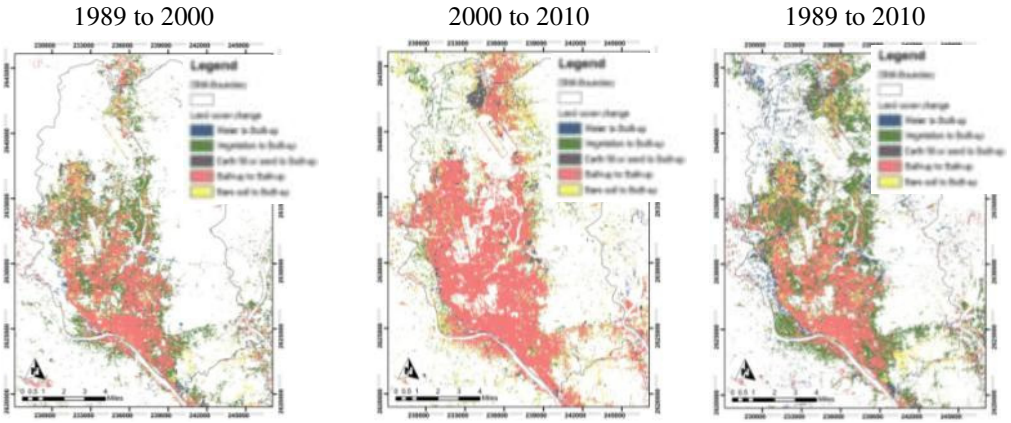

Fig. 8: Conversion of other Land Cover Types into Built-up area

Trend of Changing Land Cover Types

Figure 9 draws the attention to the trend of land covers type changing. All types of land-cover growth rates are changeable in either negative or positive rates except the Built-up area. Only Built-up area is increasing in a constant positive rate. In Figure 9, a linier trend line is added and an equation is also derived for the future estimation of Built-up area. The co-relational value, r^2 of this equation is 0.999. Value of r^2 indicates that the variable of this linear equation is highly co-related.

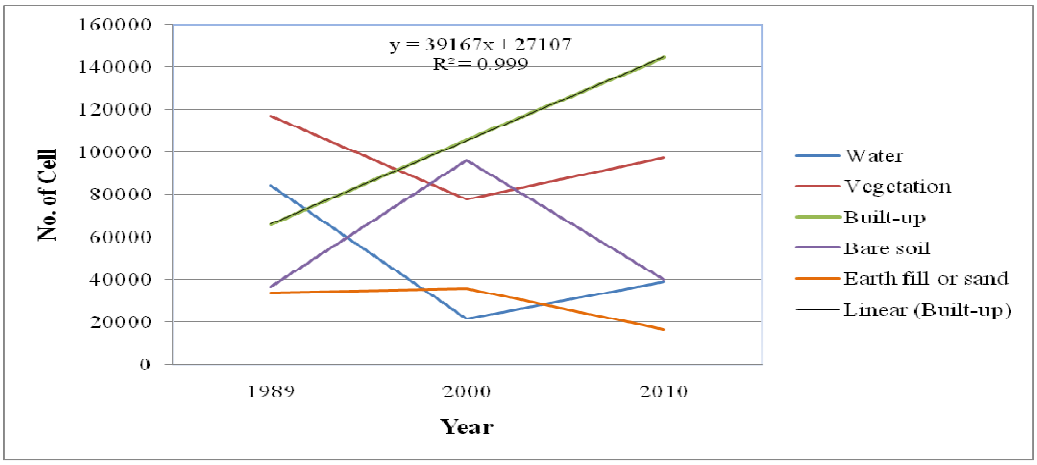

Fig. 9: Trend of land cover change over 1989 to 2010

Relationship of LST and LC

The LST due to Land cover type can be changed for pattern and density of land cover type. The spectral resolution of the Lansat TM/ETM+ images are 30m. So 900m² areas do not contain the same LC property. Greater percentage of Land type determines what will be the LC type for the pixel of Landsat image. For this reason, same type of LC's LST can be varied for same year. Again the LST value of year 2000 is higher than others because of seasonal variation. The derived mean LST of different LC type has been plotted in Figure 10, where the LST line of the year, 1989 shows almost a liner line among Built-up, Earth fill or sand and bare soil. But the vegetation has

lower LST value than other categories. In 2000, the LST line is abrupt and the Built-up LC retains more heat than other land cover classes. The mean LST of Built-up is 30.65°C which is highest LST in the Graph. Whereas the second highest heat contains the earth fill or sand type land cover and its mean LST is 30.44°C. Bare soil and water are the other land covers which are 28.62 and 27.19°C respectively. In the year 2010 the LST character is found different than 2000. Earth fill or sand land cover type is the highest temperature which is 29.72°C. But vegetation land has the low LST value. It is concluded form the above discussion that LST of vegetation value is always lower than other categories and Built-up or Earth fill or sand have the higher LST than others.

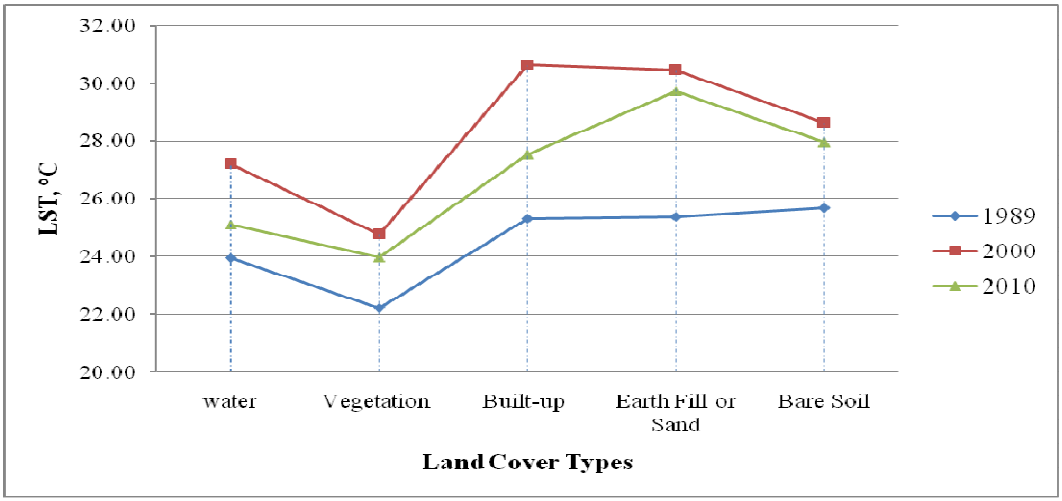

Fig. 10: Relationship between LC and mean LST

Relationships between the NDVI and LST

The relationship of LST and NDVI of different period is shown in the simulated graph 3.3, 3.4 and 3.5. Graph 3.3 represents the relationship between the NDVI and LST of year 1989. In this year the highest positive NDVI value is about 0.65 and most of the Pixel value is plotted in the positive site. The density of positive NDVI value indicates that the more probability of available of vegetation, so the vegetation density of this year is found high. The trend line of LST is negative Co-related with vegetation. Form the simulated Graph 3.4 it is found that the density of the cell value is more in the Negative portion of NDVI value. So it indicates that the less probability of available of vegetation and negative NDVI value represents highest LST value in the simulated graph. From the graph 3.5 it is found that the value of NDVI is about 0.5 and the density of the cell value is found between the NDVI ranges of -0.1 to 0.15 in the simulated graph which indicate that the density of vegetation is low. From those graph it is clear that the LST of different year is decreasing with the increasing value of NDVI as well as vegetation. So, categories of vegetation land impact on LST.

Relationships between the NDBI and LST

The relationship of the NDBI and LST is shown in the simulated graphs in Figures 11 to 16. The graphs in these figures indicate that the LST is increasing with the increasing value of NDBI. Positive value of NDBI represents the Built-up area, Bare soil and Earth fill or sand. From Figure 11, it is found that desity of the cell vule is between the range of -0.15 to 0.23 and the LST trend line is less slopy than other simulated NDBI graphs. The simulated Graphs in Figures 12 and 13 show more sloppy trend line than year 1989 and the cell desity is increased between the NDBI range of 0.1 to 0.35. Generally, the range of 0.1 to 0.35 is sensitive for Built-up area. so it can be conculed that LST is incresing with the grownup Built-up areas.

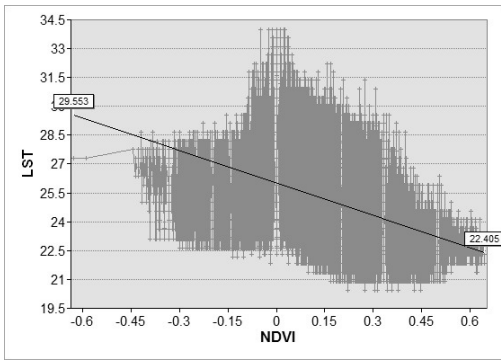

Fig. 11: Relationship of NDVI and LST, 1989

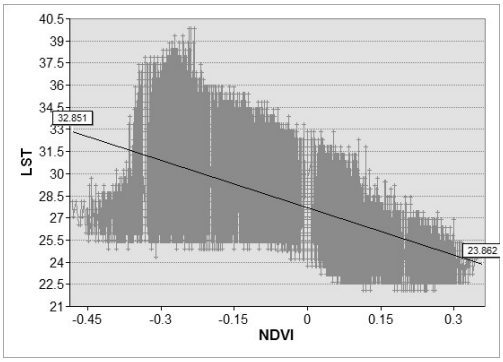

Fig. 12: Relationship of NDVI and LST, 2000

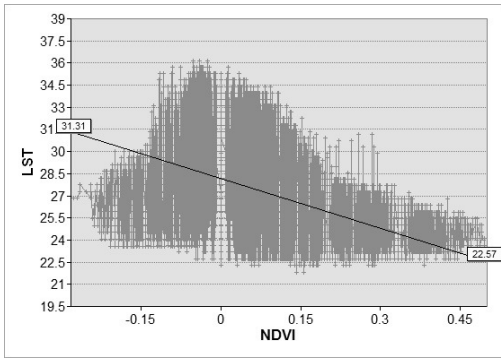

Fig. 13: Relationship of NDVI and LST, 2010

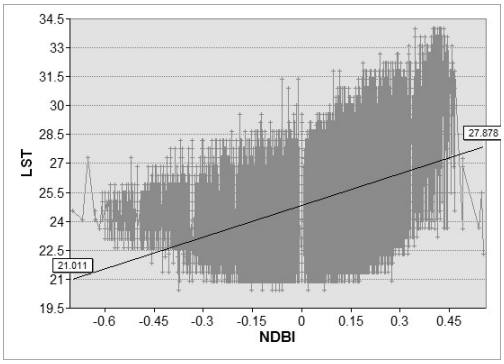

Fig. 14: Relationship of NDBI and LST, 1989

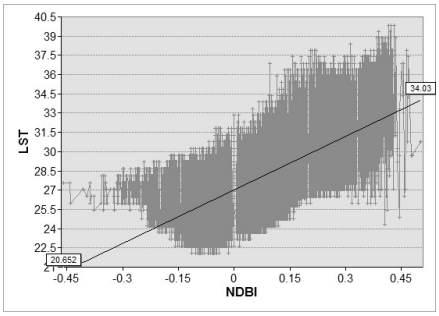

Fig. 15: Relationship of NDBI and LST, 2000

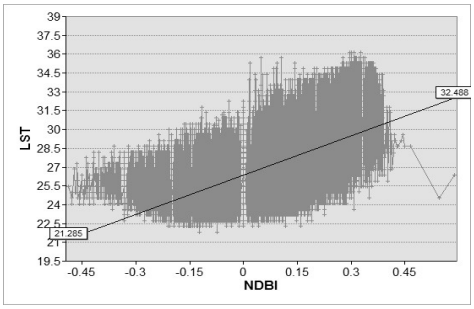

Fig. 16: Relationship of NDBI and LST, 2010

Major Findings

The major findings of the study are discussed here. Land covers (LC) of DMA have changed rapidly during the period of 1989 to 2010. Category of Water land is decreasing (-13.42%) in highest rate in this period. On the other hand, category of Built-up is grown up (23.18%) in constant growth rate during this period. A liner equation is derived for Built-up area which co-relational value r^2 is 0.999. From the analysis of NDBI and LST, it is found that the LST value is increasing with the grown built-up areas. So it creates the Urban Heat Island Effect. If the built up area is increased in this rapid growth rate, it adversely affect on microclimate.

It is found that Categories of Built-up area is increased in core center city during the period of 1989 and 2000 and highest amount of vegetation land (33.17km²) is converted to Built-up area in this period. But it is grown up more spread out within DMA during the period of 2000 to 2010.

Firstly, the categories of water land are converted into Earth fill or sand / Bare soil then it is converted into Built-up area.

Average LST is correlated with the LC changing. NDVI such as vegetation is also effect on LST. In 2000 the highest average LST of Built-up area is found because of low vegetation density. The LST of built-up is comparatively low in the other years than other LC types because of better vegetation density.

Conclusions

This report has assessed the LST change of DMA area with the transition of LC during the period of 1989 to 2010 using remote sensing image-based analysis. Analysis to LC and LST indicates that LST is negatively correlated with the NDVI but positively related with NBVI. It is also found that LST is increasing day by day because of urban development such as increasing Built up area and Earth fill or sand. It is important to control the LST otherwise the micro climate has been badly affected. Natural hazard like heat stress, flood, erratic rainfall etc. will be the cause of this increasing LST. This can also negatively affect of our economy of the country. If the changing LST is going on in this way, it is difficult to face the future unexpected natural hazard as well as loss the livable environment for living.

References

Alam, M. and Rabbani, M. G. 2007. "Vulnerabilities and responses to climate change for Dhaka" *Environment & Urbanization,* SAGE 19(1) 81–97.

Atkinson, B.W. 2002. "Numerical modeling of urban heat-island intensity" Department of Geography, Queen Mary, University of London, London E1 4NS, U.K.

Bangladesh Bureau of Statistics (BBS), 1997. *Bangladesh Population Census 1991 Urban Area Report* Dhaka: Ministry of Planning, Bangladesh.

Bangladesh Bureau of Statistics (BBS), 2003. *Population Census 2001, National Report (Provisional)* Dhaka: Ministry of Planning., Bangladesh.

Becker, F. and Li, Z.L. 1995. "Towards a local split window method over land surface" *Remote Sensing* 3 17–33.

Cao, L., Li, P., Zhang, L. and Chen, T. 2008. "Remote sensing image-based analysis of the relationship between urban heat island and vegetation fraction" The International Archives of the Photogrammetry, Remote Sensing and Spatial Information Sciences, Vol. XXXVII Part B7, Beijing.

Chen, X., Zhao, H.M., Li, P.X. and Yin, Z.Y. 2006. "Remote sensing image-based analysis of the relationship between urban heat island and land use/cover changes" *Remote Sensing of Environment* 104 (2006) 133–146

Channg, K.T. 2008. *Introduction to Geographic Information Systems* Tata MaGraw Hill Education Private Ltd., new Delhi, India(Fourth edition).

Dixon, P.G. and Mote, T.L. 2003. "Patterns and causes of Atlanta's urban heat island initiated precipitation" *Journal of Applied Meteorology* 42(9) 1273-1284.

Dickinson, R. E. 1994. Satellite systems and models for future climate change. Future Climates of the World: A Modelling Perspective, A. Henderson-Sellers, Ed., 16, World Survey of Climatology, Elsevier, 27.

Dewan, A. M., Yamaguchi, Y. 2009. "Land use and land cover change in greater Dhaka, Bangladesh: using remote sensing to promote sustainable urbanization" *Applied Geography* 29(3) 390-401.

Dougherty, J., Kohavi, R. and Sahami, M. 1995. "Supervised and unsupervised discretization of continuous features" Prieditis, A. and Russell, S. eds., Machine Learning: Proceedings of the Twelfth International Conference, Morgan Kaufmann Publishers, San Francisco, USA

Erdas Imagine Manual, 2006. Leica Geosystems Geospatial Imaging, LLC, USA

Hossain, S. 2008. "Rapid urban growth and poverty in Dhaka city" *Bangladesh e-Journal of Sociology* 5(1).

Ifatimehin, O. O., Ishaya, S. and Fanan, U. 2010. "An analysis of temperature variations using remote sensing approach in Lokoja area, Nigeria" *Production Agricultural and Technology* 6(2) 35-44 , ISSN: 0794-5213, Nasarawa State University, Keffi, Nigeria.

Lillesand, T.M. and Kiefer, R.W. 1994. "Remote sensing and image interpretation", New York

Kukla, G., Gavin, J. and Karl, T. R. 1986. 'Urban Warming' *J. Clim. Appl.Meteorol.* 25 1265–1270.

Kriegler, F.J., Malila, W.A., Nalepka, R.F. and Richardson, W. 1969. "Preprocessing transformations and their effect on multispectral recognition" Proceedings of the sixth International Symposium on Remote Sensing of Environment, University of Michigan, Ann Arbor, MI, pp. 97-131.

Mayer, H., Matzarakis, A. and Iziomon, M.G. 2003. "Spatio-temporal variability of moisture conditions within the urban canopy layer" *Theor. Appl. Climatol*. 76 165-179.

Majuire, DJ (n.d.) An overview and definition of GIS. URL:http://lidecc.cs.uns.edu.ar/~nbb/ccm/downloads/Literatura/OVERVIEW%20AND%20DEFINITION%20OF%20GIS.pdf (Accessed : 06/06 /2012)

NASA, 2010. Landsat 7 Science Data Users Handbook

URL: http://landsathandbook.gsfc.nasa.gov/pdfs/Landsat7_Handbook.pdf (Accessed: 12/06/2010)

Nasrallah, H. A. and Balling, R. C. 1993. 'Spatial and temporal analysis of middle eastern temperature changes' *Clim. Change* 25 153–161.

Nichol, J., Wong, M., Sing , F., Christopher, L. and Kenneth, K. M. 2006. "Assessment Of Urban Environmental Quality In A Subtropical City Using Multispectral Satellite Images" *Environment and Planning B: Planning and Design* 33 39 – 58.

Oxford dictionary, 2010. *Oxford* University Press, UK.

Rabbani, Md. G. 2010. "Climate Change Vulnerabilities For Urban Areas In Bangladesh: Dhaka As A Case" ICLEI, Bone, Germany. URL:http://resilient-cities.iclei.org/fileadmin/sites/resilient-cities/files/docs/B4-Bonn2010-Rabbani.pdf

Rahman, Atiq and Mallick, DL(n.d.) Climate change impacts on cities developing countries: A case study of dhaka , C40 Tokyo conference on climate change adaptation measures for sustainable low Carbone cities, Japan.

URL: http://www.kankyo.metro.tokyo.jp/en/attachement/dl_mallick.pdf(Accessed: 08/10/2012)

Sobrino, J. A., Jimenez-Munoz, J. C., El-Kharraz, J., Gomez, M., Romaguera. M. And Soria, G. 2004. "Single-channel and two-channel methods for land surface temperature

retrieval from DAIS data and its application to the Barrax site" *International Journal of Remote Sensing* 25(1) 215-230.

United State Geological Survey (USGS), 2010. URL: http://landsat.usgs.gov (Accessed: 06/08/2011)

Voogt, J.A. and Oke, T.R. 2003. 'Thermal remote sensing of urban climates' *Remote Sensing of Environment* 86 (2003) 370–384

Weng, Q. 2001. "A Remote Sensing-GIS Evaluation Of Urban Expansion And Its Impact On Surface Temperature In The Zhujiang Delta, China" *International Journal of Remote Sensing* 22(10) 1999–2014.

Wood, F. B. 1988. 'Comment: On the Need for Validation of the Jones et al. Temperature Trends with Respect to Urban Warming' *Clim. Change* 12 292–312.

Wilford, john and Creasey, john 2002. "Landsat thematic mapper" *Geophysical and remote sensing methods for regolith exploration*, CRCLEME open file report 144, pp 6-12.

World Urbanization Prospects (WUP): The 2011 Revision, 2012. Department of Economic and Social Affairs, Population Division, United Nations, New York. URL: http://esa.un.org/unup/pdf/WUP2011_Highlights.pdf (Accessed: 15/06/2012)

World City information (WCI), 2012. URL: http://www.city-infos.com/dhaka/ (Accessed: 12/09/2012)

Zha, Y., Gao, J., & Ni, S. 2003. "Use of normalized difference built-up index in automatically mapping urban areas from TM imagery" *International Journal of Remote Sensing* 24(3) 583−594.

Zhang, Z., Ji, M., Shu, J., Deng, Z. and Wu, Y. 2008. "Surface Urban Heat Island In Shanghai, China: Examining The Relationship Between Land Surface Temperature And Impervious Surface Fractions Derived From Landsat ETM+ Imagery" The International Archives of the Photogrammetry, Remote Sensing and Spatial Information Sciences, Vol. XXXVII Part B8, Beijing.

Zhang, J., Lia, Y. and Wang, Y. 2007. "Monitoring the Urban Heat Island and the Spatial Expansion: Using Thermal Remote Sensing Image Of ETM+ Band6" paper presented at Geoinformatics 2007: Remotely Sensed Data and Information, 25 May, Nanjing, China.

Yuan, F. and Bauer, M. E. 2007. "Comparison Of Impervious Surface Area and Normalized Difference Vegetation Index As Indicators of Surface Urban Heat Island Effects in Landsat Imagery" *Remote Sensing of Environment* 106 375–386.

Xian, G. and Crane, M. 2005. "Evaluation of Urbanization on the Influences on Urban Climate with Remote Sensing and Climate Observations" paper presented at 5th International Symposium Remote Sensing of Urban Areas, 14-16 March, Tempe, AZ, USA.